



# Meloxicam Inhibited the Proliferation of LPS-Stimulated Bovine Endometrial Epithelial Cells Through Wnt/ $\beta$ -Catenin and PI3K/AKT Pathways

Luying Cui<sup>1,2†</sup>, Yang Qu<sup>1,2†</sup>, Hele Cai<sup>1,2</sup>, Heng Wang<sup>1,2</sup>, Junsheng Dong<sup>1,2</sup>, Jun Li<sup>1,2</sup>, Chen Qian<sup>1,2</sup> and Jianji Li<sup>1,2\*</sup>

<sup>1</sup> College of Veterinary Medicine, Yangzhou University, Jiangsu Co-innovation Center for Prevention and Control of Important Animal Infectious Diseases and Zoonoses, Yangzhou, China, <sup>2</sup> Joint International Research Laboratory of Agriculture and Agriproduct Safety of the Ministry of Education, Yangzhou, China

## OPEN ACCESS

### Edited by:

Haichong Wu,  
Zhejiang University, China

### Reviewed by:

Chengming Wang,  
Auburn University, United States  
Zhenlei Zhou,  
Nanjing Agricultural University, China  
Guangneng Peng,  
Sichuan Agricultural University, China

### \*Correspondence:

Jianji Li  
yzjjli@163.com

<sup>†</sup>These authors have contributed  
equally to this work and share first  
authorship

### Specialty section:

This article was submitted to  
Animal Reproduction -  
Theriogenology,  
a section of the journal  
Frontiers in Veterinary Science

Received: 04 December 2020

Accepted: 19 April 2021

Published: 09 July 2021

### Citation:

Cui L, Qu Y, Cai H, Wang H, Dong J,  
Li J, Qian C and Li J (2021)  
Meloxicam Inhibited the Proliferation  
of LPS-Stimulated Bovine Endometrial  
Epithelial Cells Through Wnt/ $\beta$ -Catenin  
and PI3K/AKT Pathways.  
Front. Vet. Sci. 8:637707.  
doi: 10.3389/fvets.2021.637707

Meloxicam is a non-steroidal anti-inflammatory drug and has been used to relieve pain and control inflammation in cows with metritis and endometritis. Meloxicam has been found to be effective in inhibiting tissue or cell growth when it is used as an anti-inflammatory therapy. However, the influence of meloxicam on bovine endometrial regeneration has not been reported. This study was to research the effect of meloxicam (0.5 and 5  $\mu$ M) on the proliferation of primary bovine endometrial epithelial cells (BEECs) stimulated by *Escherichia coli* lipopolysaccharide. The cell viability, cell cycle, and cell proliferation were evaluated by Cell Counting Kit-8, flow cytometry, and cell scratch test, respectively. The mRNA transcriptions of prostaglandin-endoperoxide synthase 1 (*PTGS1*) and *PTGS2*, Toll-like receptor 4, and proliferation factors were detected using quantitative reverse-transcription polymerase chain reaction. The activations of phosphatidylinositol 3-kinase (PI3K)/protein kinase B (AKT) and Wnt/ $\beta$ -catenin pathways were determined using western blot and immunofluorescence. As a result, co-treatment of meloxicam and lipopolysaccharide inhibited ( $P < 0.05$ ) the cell cycle progression and reduced ( $P < 0.05$ ) the cell healing rate and the mRNA level of proliferation factors as compared with the cells treated with lipopolysaccharide alone. Meloxicam decreased ( $P < 0.05$ ) the lipopolysaccharide-induced *PTGS2* gene expression. Neither lipopolysaccharide nor meloxicam changed *PTGS1* mRNA abundance ( $P > 0.05$ ). Meloxicam inhibited ( $P < 0.05$ ) the lipopolysaccharide-activated Wnt/ $\beta$ -catenin pathway by reducing ( $P < 0.05$ ) the protein levels of  $\beta$ -catenin, c-Myc, cyclin D1, and glycogen synthase kinase-3 $\beta$  and prevented the lipopolysaccharide-induced  $\beta$ -catenin from entering the nucleus. Meloxicam suppressed ( $P < 0.05$ ) the phosphorylation of PI3K and AKT. In conclusion, meloxicam alone did not influence the cell cycle progression or the cell proliferation in BEEC but caused cell cycle arrest and inhibited cell proliferation in lipopolysaccharide-stimulated BEEC. This inhibitory effect of meloxicam was probably mediated by Wnt/ $\beta$ -catenin and PI3K/AKT pathways.

**Keywords:** meloxicam, bovine endometrial epithelial cells, proliferation, lipopolysaccharide, Wnt/ $\beta$ -catenin, PI3K/AKT

## INTRODUCTION

Post-partum uterine infection is a common reproductive disease in cattle, causing an increased culling rate and huge economic losses to the breeding industry. Bovine endometritis is a common disease occurring in post-partum cows, with an incidence rate of 10–30% (1). Infections of the uterus with *Escherichia coli* precede infection by other common pathogenic bacteria via the production of lipopolysaccharide (LPS) (2, 3).

Following calving, the uterine involution includes tissue repair, endometrial regeneration, and bacteria elimination (4). The formation of new epithelium will be important in maintaining the next-round pregnancy and in re-establishing the innate defense system (5). Bovine endometrial epithelial cells (BEECs) are required in defending against *E. coli* and in repairing the epithelium (6). The vascular endothelial growth factor (VEGF) has been found to promote endometrial repair in mice and primates (7). The connective tissue growth factor (CTGF) participates in endometrial repair and has many physiological functions such as promoting angiogenesis, mitosis, and cell adhesion (8). The insulin-like growth factor and insulin-like growth factor receptor (IGFR) participate in the regulation of mitosis of endometrial epithelial cells (9). The transforming growth factor- $\beta$  (TGF- $\beta$ ) is involved in the differentiation and proliferation of many kinds of cells, initiating tissue repair (10).

The Wnt pathway is a highly conserved signal transduction cascade that regulates cell growth and proliferation. In primates and mice, the Wnt/ $\beta$ -catenin pathway is involved in endometrial repair (11, 12). The activation of the adenomatous polyposis coli/axin/glycogen synthase kinase-3 $\beta$ / $\beta$ -catenin/casein kinase 1 complex results in the dephosphorylation of  $\beta$ -catenin, which then enters the nucleus and activates downstream c-Myc, cyclin D1, and VEGF transcription to regulate cell cycle and cell proliferation (13, 14). The phosphatidylinositol 3-kinase (PI3K)/protein kinase B (AKT) signal transduction pathway participates in cell growth, proliferation, and differentiation. It has been proved that the PI3K/AKT pathway is involved in endometrial repair in human and dairy goats (15, 16).

The conventional treatment for uterine infection includes environmental disinfection, uterine irrigation, and uterine infusion with large amounts of antibiotics. Non-steroidal anti-inflammatory drugs (NSAIDs) in combination with antibiotics are used increasingly in the treatment of metritis and endometritis (17). Studies have shown that NSAIDs provide therapeutic effects such as analgesia, ovarian function recovery, and prevention and treatment of uterine inflammation (18). Meloxicam (MEL) is an NSAID that preferentially inhibits cyclooxygenase-2 (COX-2) in most animals, but this affinity has not been verified in dairy cows (19). MEL has been found to decrease the viability of breast cells in cows with mastitis, suggesting a potential side effect of MEL to bovine breast tissue (20). More experimental trials and clinical reports are required to clarify the mechanism and effect of MEL in treating bovine post-partum uterine diseases. So far, there are few studies regarding the effect of MEL on the survival and proliferation of BEEC.

The goal of this study was to reveal the influence and mechanism of MEL on BEEC proliferation. The BEEC was

treated with LPS. The changes in the cell cycle, cell scratch test, the mRNA transcriptions of prostaglandin-endoperoxide synthase 1 (*PTGS1*) and *PTGS2*, Toll-like receptor 4 (*TLR4*), and growth factors and the key proteins of Wnt/ $\beta$ -catenin and PI3K/AKT pathways were determined.

## MATERIALS AND METHODS

### Culture of BEECs

The cells were isolated as described from Dong et al. (21). Briefly, cows with no signs of genital disease or microbial infection were selected in the slaughterhouse, based on the presence of foul smell, characteristic visual appearance, and vaginal discharge (1). The uterus was collected aseptically and stored on ice at 4°C until further treatment in the laboratory. The uterine horn was cut into 3–4-cm-long tissue blocks and was washed with PBS (pH value from 7.2 to 7.4). Then the tissue blocks were transferred to 0.1% streptose (P5147, Sigma, USA) diluted with DMEM/F-12 (D8900, Sigma, USA) and digested at 4°C for 16–20 h. Under sterile conditions, the tissue block was removed, and the endometrial tissue was scraped with a sterilized scalpel. The cell suspension was centrifuged at 100  $\times$  g for 5 min and washed with PBS three times. The cells were then collected and resuspended with DMEM/F-12 containing 15% fetal bovine serum (FBS, Gibco, USA) and 50 U/ml penicillin/streptomycin, and inoculated into a 25-cm<sup>2</sup> bottle. The cells were cultured in the incubator at 37°C and 5% CO<sub>2</sub> saturation humidity. The medium was changed every 1–2 days. The primary cells could be obtained after 3–4 days.

### MEL Treatment

MEL (M3935, Sigma-Aldrich, USA) was dissolved in DMSO and stored at –20°C. It has been reported that the injection dose of 0.5 mg/kg MEL could maintain the blood concentration of 0.2  $\mu$ g/ml MEL in cows with endometritis (22). In addition, MEL was used in a bovine lymphocyte test (23, 24), which provided references for MEL concentration in this experiment. In this study, two concentrations of MEL, 0.5 and 5  $\mu$ M, were selected. First, 100 mg MEL was dissolved in 26.782 ml DMSO. Then, a 1 ml DMSO–MEL solution was added in 49 ml DMEM/F-12 for storage at –20°C. This storage concentration was 200  $\mu$ M. MEL was filtered before use. The experiment was divided into four groups: the control group, the LPS group, the MEL group, and the LPS plus MEL co-treatment (LPS–MEL) groups. According to the results of previous reports in our lab, 10  $\mu$ g/ml LPS (L2630, Sigma, USA) did not influence the cell viability of BEEC (25). Therefore, 10  $\mu$ g/ml LPS was selected for this study.

### Cell Viability Assay

The Cell Counting Kit-8 (CCK-8, Dojindo Molecular Technologies, Inc., Japan) was used to determine the effect of MEL and LPS on cell viability. The cells were seeded on 96-well plates with a density of 1  $\times$  10<sup>3</sup> cells per well and grew to 80% fusion in a 5% CO<sub>2</sub> incubator at 37°C. Then the cells were treated with 5  $\times$  10<sup>–2</sup>, 5  $\times$  10<sup>–1</sup>, 5, or 5  $\times$  10<sup>1</sup>  $\mu$ M MEL or with 10  $\mu$ g/ml LPS. CCK-8 was added into each well and incubated

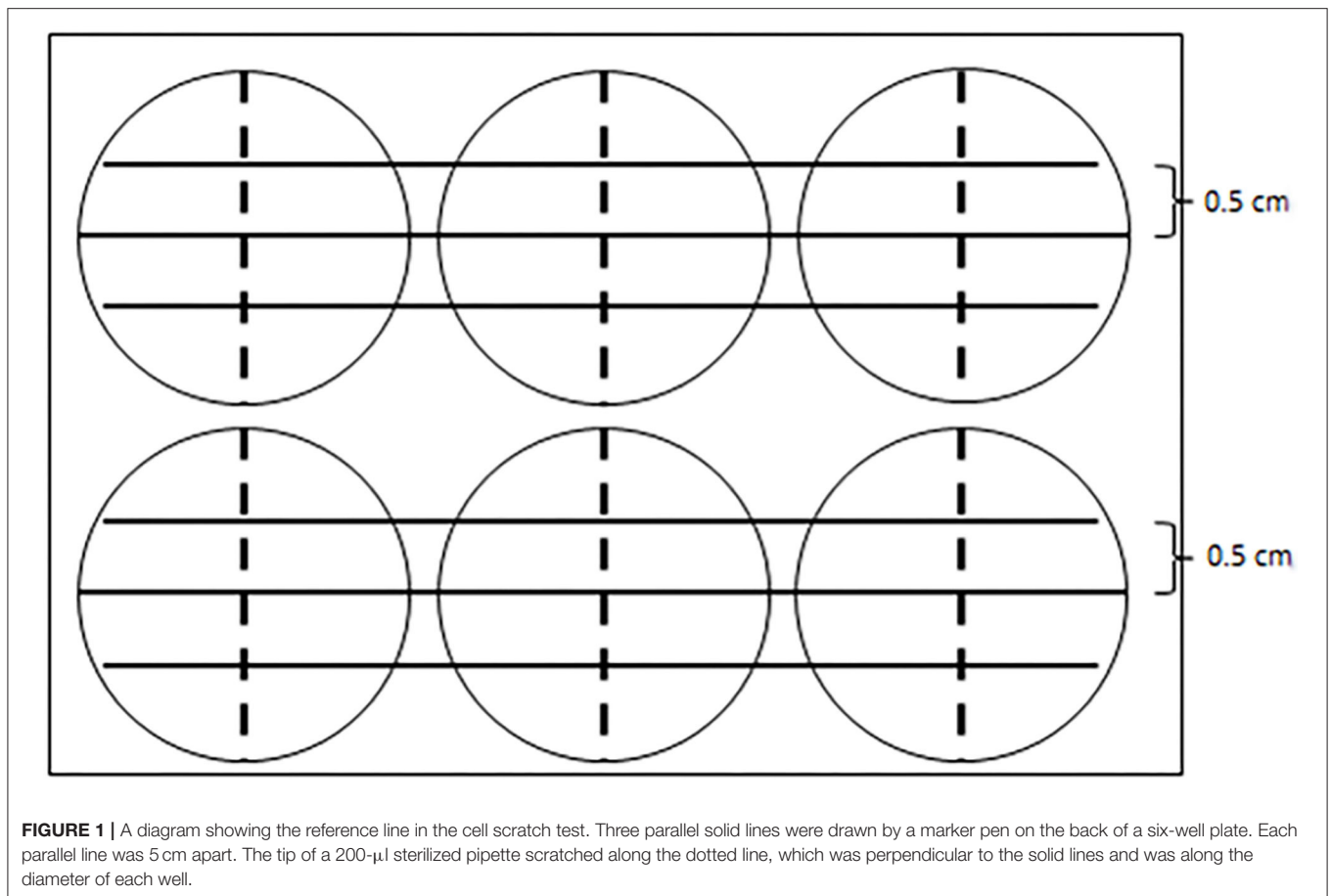


**FIGURE 1** | A diagram showing the reference line in the cell scratch test. Three parallel solid lines were drawn by a marker pen on the back of a six-well plate. Each parallel line was 5 cm apart. The tip of a 200- $\mu$ l sterilized pipette scratched along the dotted line, which was perpendicular to the solid lines and was along the diameter of each well.

**TABLE 1** | The list of primer sequences.

Gene	Forward primers	Reverse primer	Product size (bp)	Accession number
<i>ACTB</i>	CATCACCATCGGCAATGAGC	AGCACCGTGTGGCGTAGAG	156	NM_173979.3
<i>PTGS1</i>	TGCCATCCGAACCTCCATCTT	AATGTGCTTGCCTTCCAGTAC	116	NM_001105323.1
<i>PTGS2</i>	GCACAAATCTGATGTTGCATTC	AGCTGGTCTCGTTCAAATCT	80	NM_174445.2
<i>TLR4</i>	GCTCTGCCTTCACTACAGGGACT	CTGGGACACCACGACAATAACC	106	NM_174198.6
<i>VEGFA</i>	GACCCTGGTGGACATCTTCC	CACACAGGGCACACACTCC	127	NM_001316992.1
<i>CCN2</i>	AGCTGACCTGGAGGAGAACA	GTCTGTGCACACTCCGCAGA	139	NM_174030.2
<i>IGF1R</i>	TTAAATGGCCAGAACCTGAG	ATTATAACCAAGCCTCCCAC	314	NM_001244612.1
<i>TGFB1</i>	CGAGCCCTGGACACCAACTA	AGGCAGAAATTGGCGTGGTA	137	NM_001166068.1
<i>TGFB3</i>	CTGTGCGTGAATGGCTCTTG	CATCATCGCTGTCCACACCT	153	NM_001101183.1

at 37°C for 2–4 h. The optical density was then read at 450 nm using a microplate (Tecan, Austria).

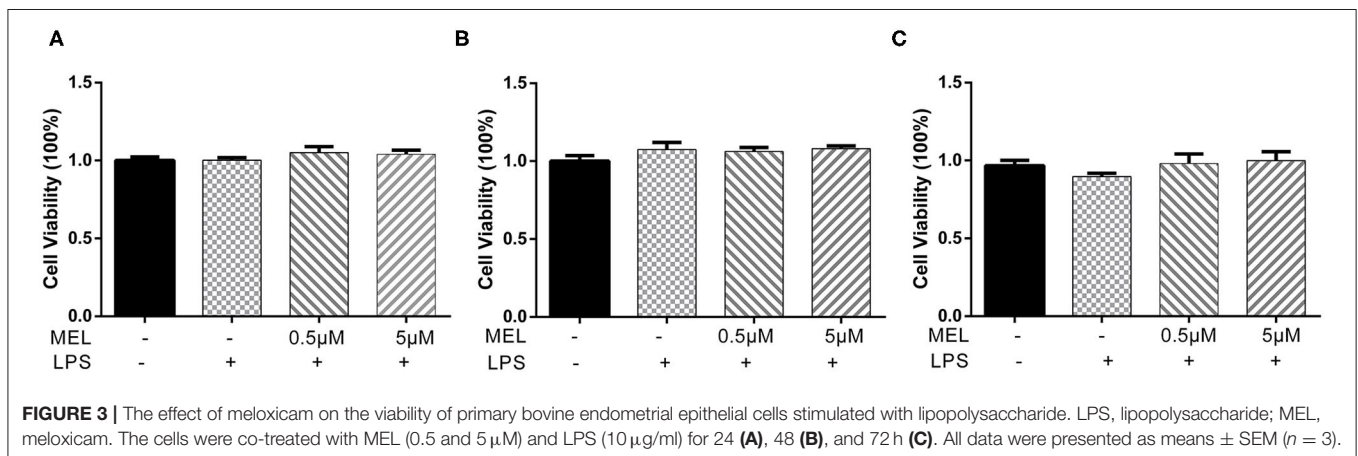
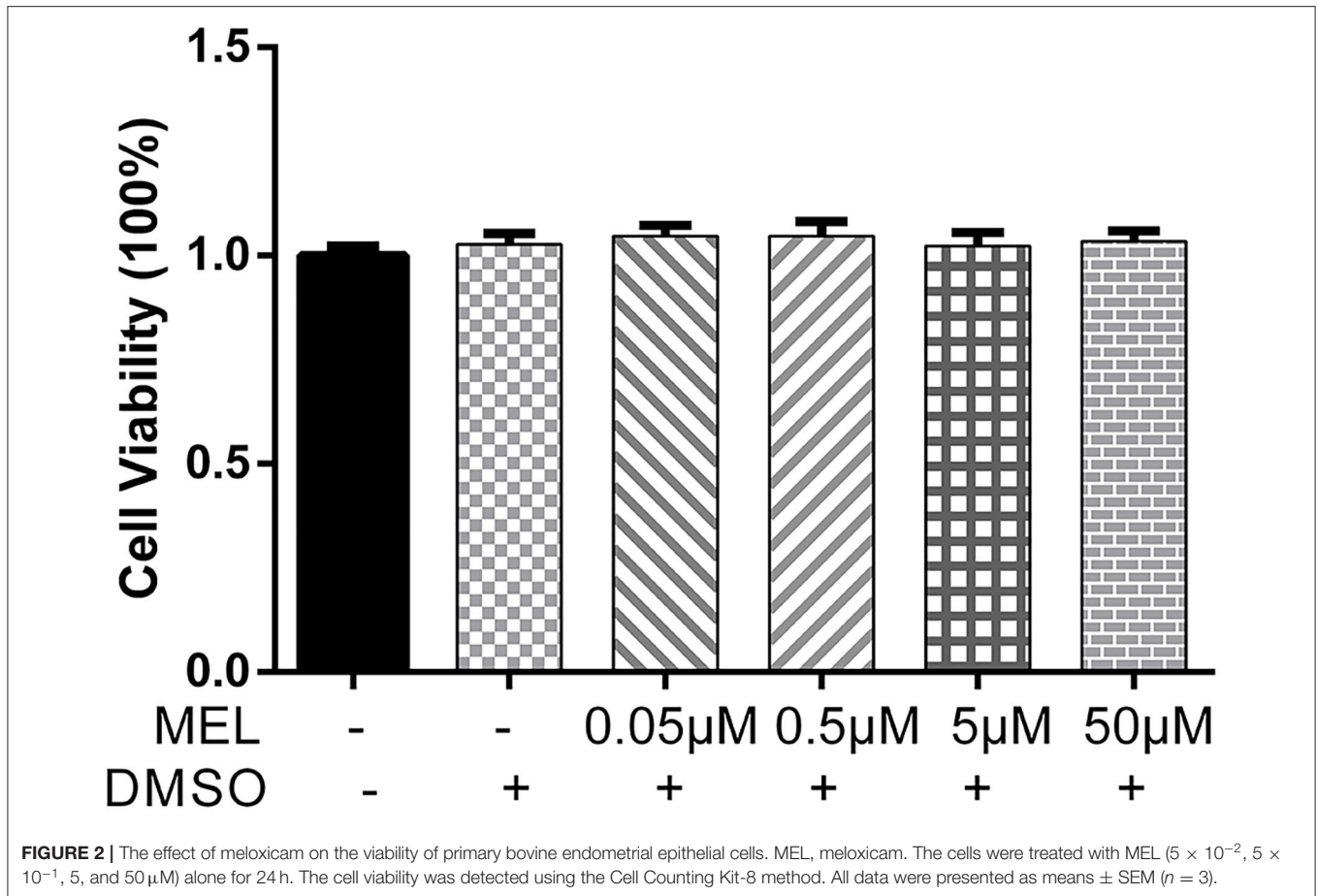
### Cell Cycling Analysis

BEEC was treated with MEL or LPS or LPS–MEL for 24 h. The cells were washed twice with cold PBS and fixed with 70% ethanol at 4°C for 12–24 h. Then the cells were washed twice with cold PBS and resuspended with RNase A and propidium iodide (C1052, Beyotime, China) in the dark at 37°C for 30 min. Cell cycle was detected by flow cytometry (LSRFortessa, BD Biosciences, USA) and was analyzed by FlowJo software 7.6

(Becton, Dickinson, and Company, Ashland, USA) to obtain the relative number of cells in each phase of the cell cycle.

### Cell Scratch Test

Before cell culture, three parallel lines, each 0.5 cm apart, were drawn on the back of a six-well plate using a marker pen. The cells were then seeded on this plate with a density of  $1 \times 10^6$  cells per well and were cultured overnight in a cell incubator with 5% CO<sub>2</sub> at 37°C. The cell scratch test started when the cells reached 90% fusion. The cells were scratched by using the tip of a 200  $\mu$ l sterilized pipette. This scratching line was perpendicular

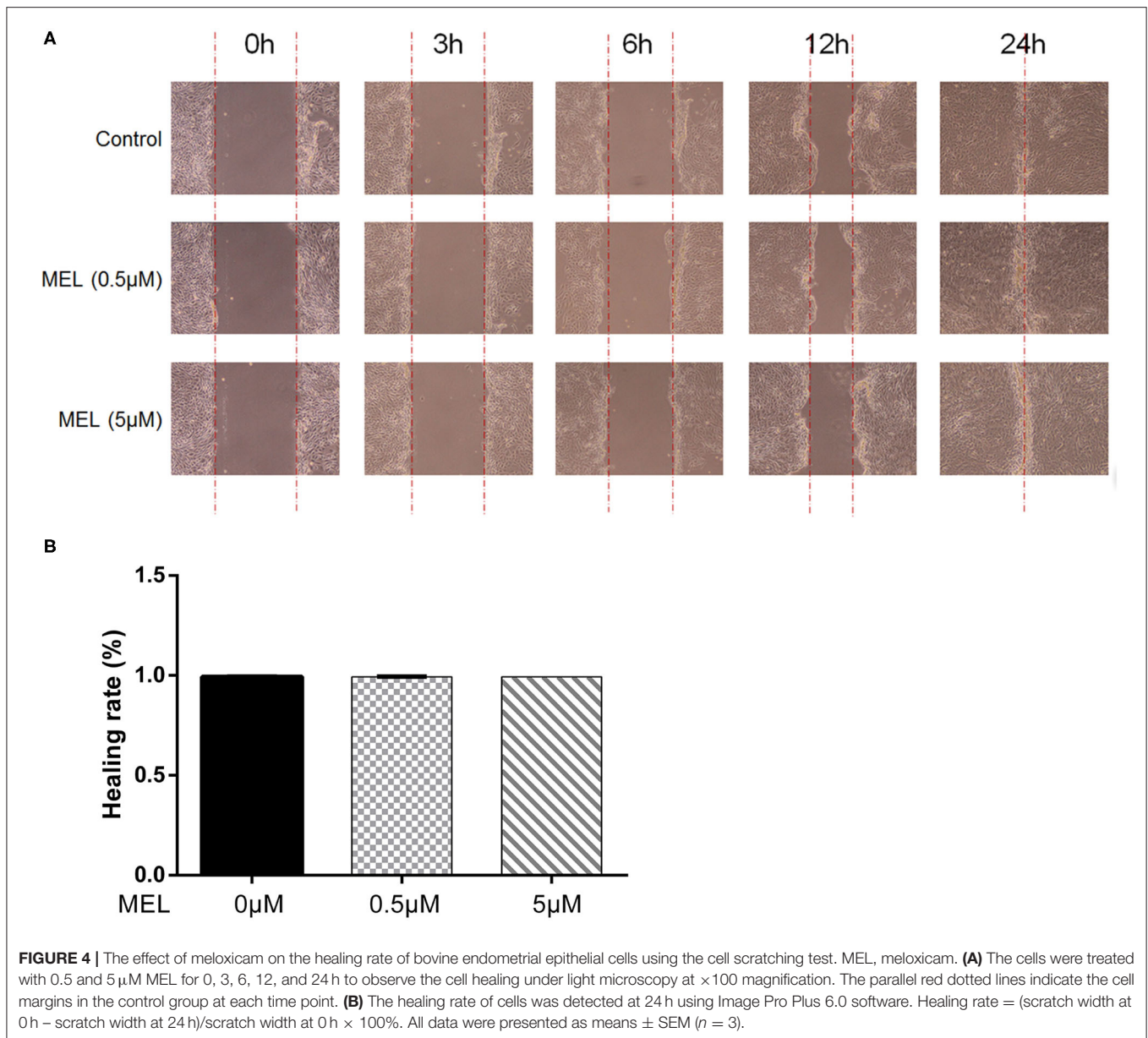


to the previous three lines and was along the diameter of the well. The cells were quickly washed with PBS at least three times until no cell was visible at the scratch microscopically. Then the DMEM/F-12 containing LPS or MEL was added to the well. The cell treatments were as follows: LPS, MEL (0.5 or  $5 \mu\text{M}$ ), or LPS–MEL (0.5 or  $5 \mu\text{M}$ ).

The six-well plate was observed under the inverted microscope at  $\times 100$  magnification. Photos were taken

immediately after the scratching (0 h) and at 3, 6, 12, and 24 h at fixed positions, which were localized with the help of the three parallel lines (Figure 1). The photos were analyzed by Image-Pro Plus software 6.0 (Media Cybernetics, Rockville, USA). The healing rate of the scratch reflects cell proliferation. The calculations were as follows:

$$\text{Scratch width} = \text{scratch area} / \text{scratch length}$$

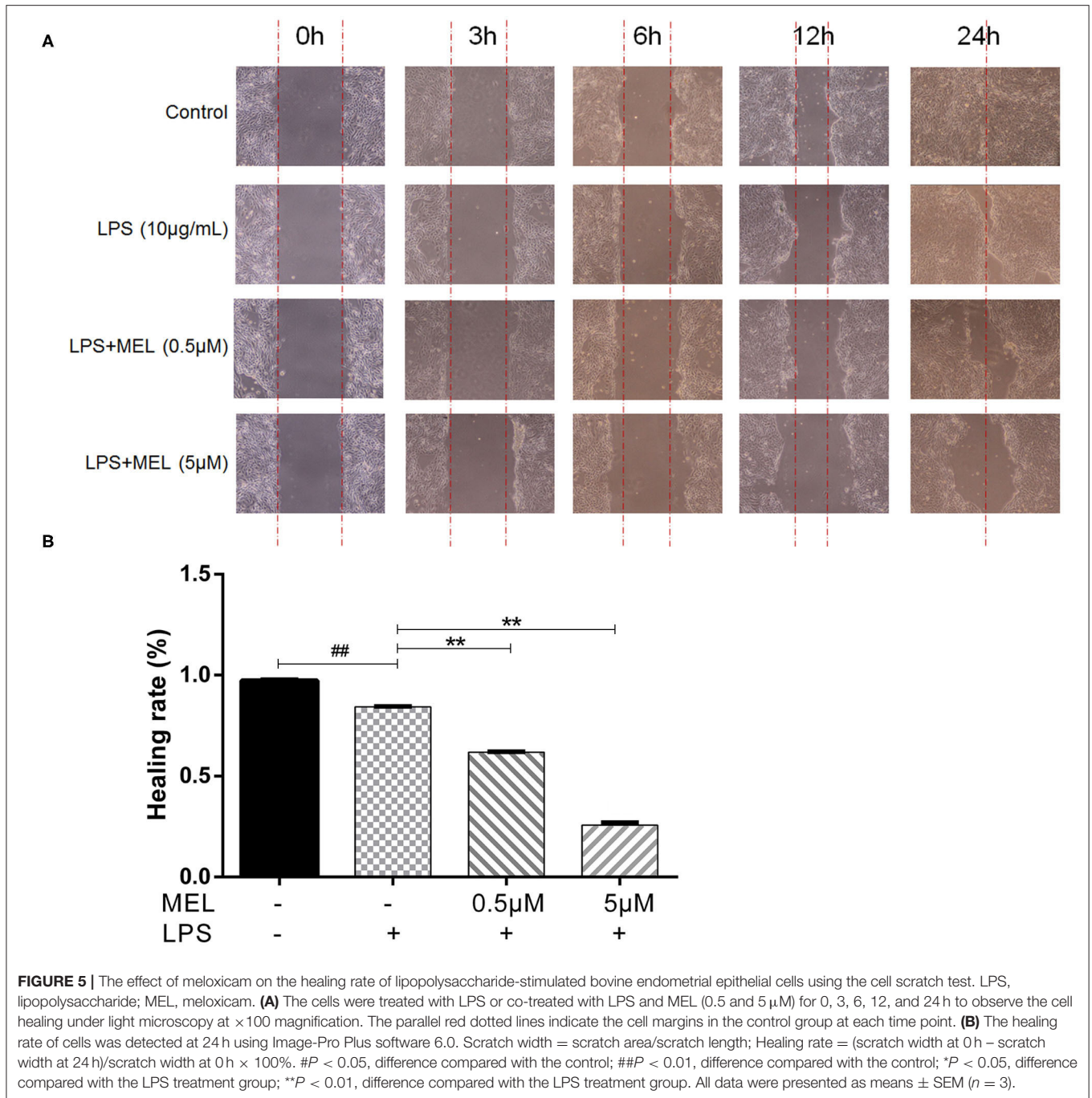


Healing rate = (scratch width at 0 h – scratch width at various time points)/scratch width at 0 h  $\times$  100%

### RNA Extraction and Quantitative Reverse-Transcription Polymerase Chain Reaction

The cells were seeded into a six-well plate and were treated with LPS, MEL (0.5 and 5  $\mu$ M), or LPS–MEL (0.5 and 5  $\mu$ M) for 0, 3, 12, and 24 h. Total RNA was extracted using TRIzol reagent (ET111, TRAN, China) according to the manufacturer's instruction. A Nanodrop 2000 spectrophotometer (Thermo, USA) was used to detect the quantity and purity of the RNA. The absorption ratio (A260/A280) was determined to be between

1.8 and 2.1. The total RNA was reverse-transcribed into cDNA by a PrimeScript RT reagent kit gDNA eraser (DRR047A, Takara, Japan). The cycle conditions were as follows: 95°C for 2 min; 95°C for 5 s and 60°C for 34 s, 40 times; 95°C for 15 s; 60°C for 5 s; 60–95°C, 0.5°C gradient heating. The reaction system included 10  $\mu$ l SYBR Premix Ex Taq<sup>TM</sup> II (RR820A, TaKaRa, Japan), 1  $\mu$ l of each primer, 1  $\mu$ l cDNA template in a final volume of 20  $\mu$ l per reaction. The  $2^{-\Delta\Delta CT}$  method was used to calculate the relative abundances of mRNA transcripts (26). Each group was repeated three times. The  $\beta$ -actin (*ACTB*) was used as the internal control. The primers were designed according to the mRNA sequences of bovine *ACTB*, *PTGS1*, *PTGS2*, *TLR4*, *VEGFA*, cellular communication network factor 2 (*CCN2*), insulin-like growth factor 1 receptor (*IGF1R*), *TGFBI*, and

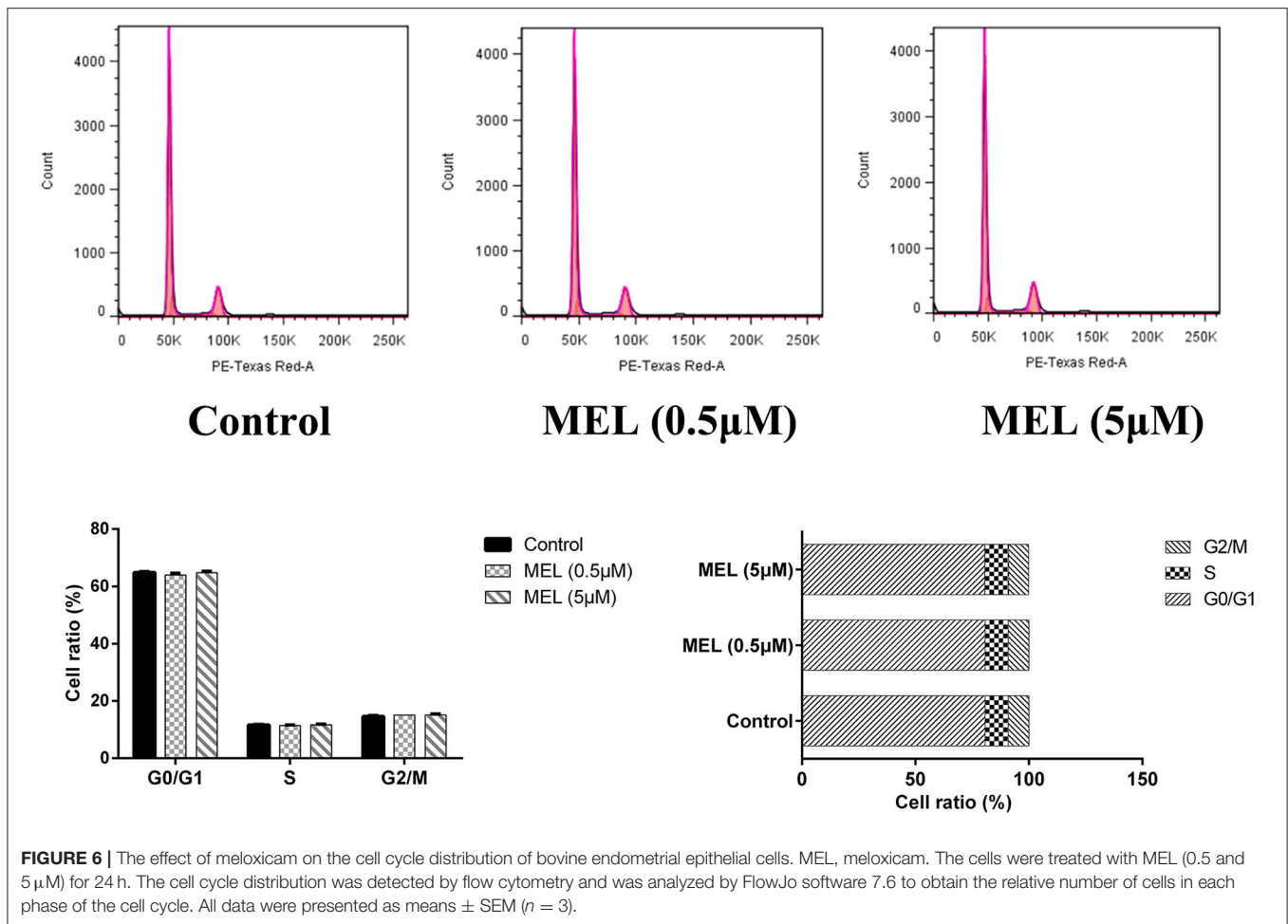


*TGFB3* published in GenBank. A single product was amplified by each primer pair. All the polymerase chain reaction (PCR) products were purified and sequenced (TsingKe Biotech, Beijing, China), and the sequence results were analyzed using BLAST and compared to the GenBank database (<http://blast.ncbi.nlm.nih.gov/blast.cgi>). The primer sequences are shown in **Table 1**.

### Western Blot Analysis

BEECs were treated with LPS, MEL (0.5 and 5 µM), or LPS–MEL (0.5 and 5 µM). The total protein was extracted and quantified

by a bicinchoninic acid protein assay kit (P0010, Beyotime, China). The protein (20–30 µg) was separated by 10% SDS–polyacrylamide gels and was transferred to the polyvinylidene difluoride (PVDF) membrane (Millipore, Germany). The PVDF membrane was incubated in 5% skimmed milk diluted by TBST (0.05% Tween-20 Tris-HCl buffer) to prevent its binding to non-specific protein. The primary antibody used for incubation included β-catenin, c-Myc, cyclin D1, glycogen synthase kinase-3β (GSK-3β), p-PI3K, PI3K, p-AKT, AKT, and β-actin at 4°C overnight. Then the PVDF membrane was incubated with



horseradish peroxidase (HRP)-conjugated secondary antibody (diluted with 5% skimmed milk to 1:2,000) for 1 h at room temperature. Proteins were detected using a chemiluminescence assay. The antigen-antibody complex was visualized using a HRP substrate (Millipore, Billerica, MA, USA) and the ChemiScope 5300 Pro CCD camera (Clinx Science Instruments, Shanghai, China). The band intensity quantification was analyzed by Quantity One software (Bio-Rad, CA, USA). The primary antibodies of c-Myc (#5605), cyclin D1 (#2978), p-PI3K (#4228), PI3K (#4292), p-AKT (#4060), AKT (#4691), and  $\beta$ -actin (#4970) were purchased from Cell Signaling Technology. The  $\beta$ -catenin primary antibody (#ab32572) was purchased from Abcam (UK), and the GSK-3 $\beta$  primary antibody (#A2081) was purchased from ABclonal (China).

### Immunofluorescence Staining

The cells were seeded on a 24-well cell culture plate and were treated with LPS, MEL (0.5  $\mu$ M), or LPS-MEL (0.5 and 5  $\mu$ M) for 15 min. Then the cells were fixed with 4% paraformaldehyde for 15 min. After washing with PBS, the membrane was penetrated with 0.4% Triton X-100 (ST797, Beyotime, China) for 15 min. The cells were washed with PBS three times and were blocked by 5% BSA for 1.5 h at room temperature. The cells were incubated

with anti- $\beta$ -catenin (all at 1:250 in 5% BSA) at 4°C overnight. After PBS washings for three times, the cells were incubated with an FITC-conjugated secondary antibody (A0423, Beyotime, China) for 1.5 h at room temperature. The nuclei were stained with DAPI (C1005, Beyotime, China). Finally, the cells were visualized with a fluorescence microscope (Leica TCS SP8, Leica Corporation, Germany).

### Statistical Analysis

The experiment was repeated at least three times. All the data were analyzed using SPSS 21.0 software (IBM, NY, USA). Statistically significant differences throughout this study were calculated by one-way ANOVA, followed by Dunnett's test. The data were shown as means  $\pm$  standard error of means (SEM). A bilateral  $P < 0.05$  was considered statistically significant.

## RESULTS

### BEEC Viability

The CCK-8 method was used to detect the effect of MEL on BEEC viability. The viability of BEEC was not influenced ( $P > 0.05$ ) by various concentrations ( $5 \times 10^{-2}$ ,  $5 \times 10^{-1}$ , 5, and  $5 \times 10^1$   $\mu$ M) of MEL (Figure 2).

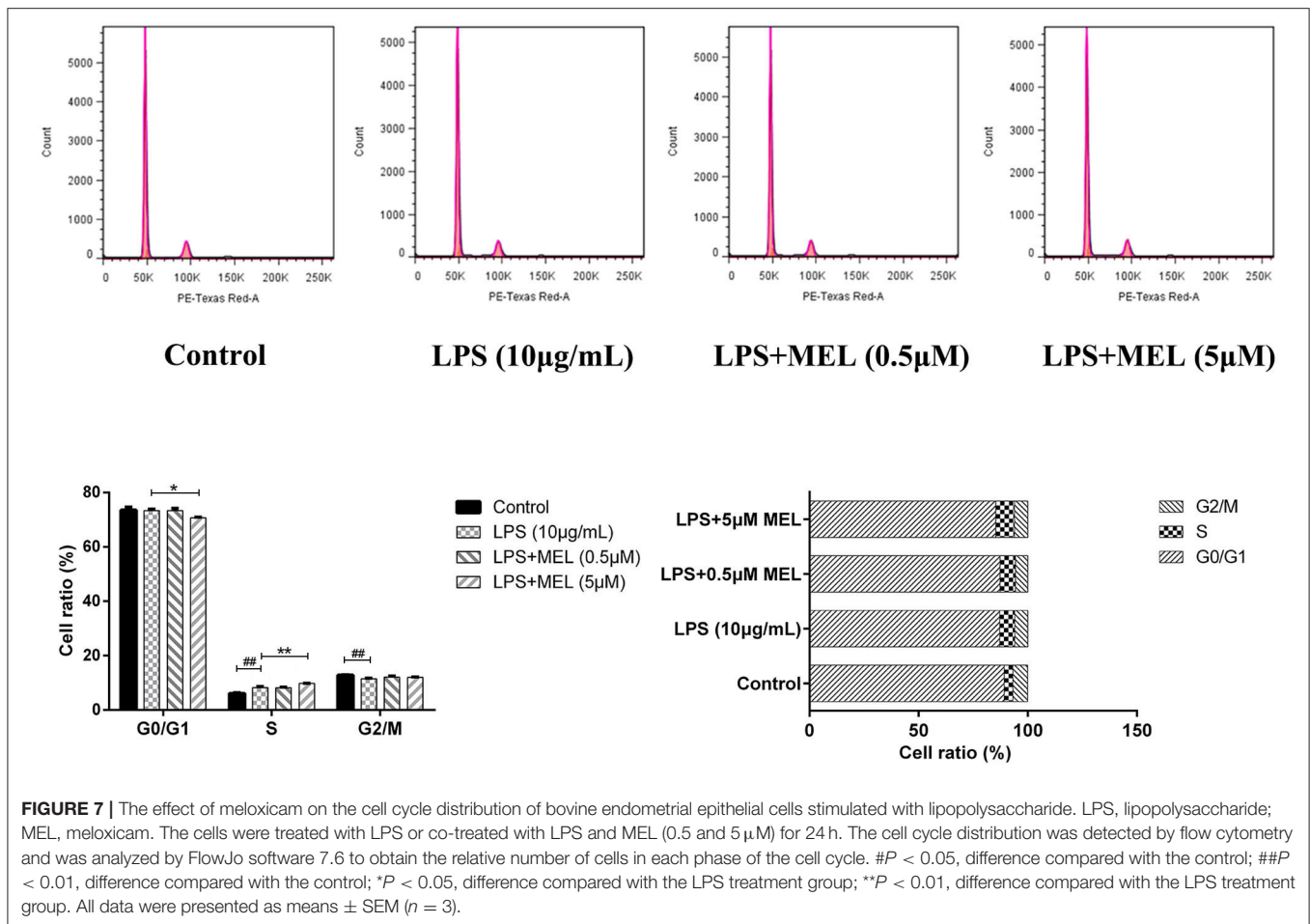


**FIGURE 7 |** The effect of meloxicam on the cell cycle distribution of bovine endometrial epithelial cells stimulated with lipopolysaccharide. LPS, lipopolysaccharide; MEL, meloxicam. The cells were treated with LPS or co-treated with LPS and MEL (0.5 and 5 μM) for 24 h. The cell cycle distribution was detected by flow cytometry and was analyzed by FlowJo software 7.6 to obtain the relative number of cells in each phase of the cell cycle. # $P < 0.05$ , difference compared with the control; ## $P < 0.01$ , difference compared with the control; \* $P < 0.05$ , difference compared with the LPS treatment group; \*\* $P < 0.01$ , difference compared with the LPS treatment group. All data were presented as means  $\pm$  SEM ( $n = 3$ ).

As shown in **Figure 3**, no difference ( $P > 0.05$ ) was observed in the cell viability between the cells treated with only LPS and the cells co-treated with LPS and MEL (0.5 and 5 μM).

### BEEC Scratch Test

The effect of MEL on the healing rate of BEEC was detected using the scratching test. There was no difference ( $P > 0.05$ ) in cell migration at 24 h in cells treated with 0.5 or 5 μM MEL alone (**Figure 4**). The cell healing rate of the LPS group was lower ( $P < 0.01$ ) than that of the blank control group. Compared with the LPS group, the cell healing rate decreased ( $P < 0.01$ ) in the LPS–MEL groups (**Figure 5**).

### BEEC Cycle

The influence of MEL on the cell cycle of BEEC was determined using flow cytometry. As shown in **Figure 6**, MEL had no effect ( $P > 0.05$ ) on the number of cells in each cell cycle. After treatment with LPS for 24 h, the number of cells increased ( $P < 0.01$ ) in the S phase and decreased ( $P < 0.01$ ) in the G2 phase, indicating the cell cycle arrest in the S phase. After treatment with LPS and MEL for 24 h, the number of cells decreased ( $P < 0.01$ ) in the G1 phase and increased ( $P < 0.01$ ) in the S phase, suggesting the cell cycle arrest in the G0/G1 phase (**Figure 7**).

### Gene Expressions of *PTGS1*, *PTGS2*, *TLR4*, and Growth Factors in BEECs

The effects of MEL on the gene expressions of *PTGS1*, *PTGS2*, *TLR4*, and the growth factors (*VEGFA*, *CCN2*, *IGF1R*, *TGFB1*, and *TGFB3*) were detected using quantitative reverse-transcription PCR. As shown in **Figures 8A,B**, compared with the blank control, the gene expressions of *PTGS2* and *TLR4* increased ( $P < 0.01$ ) after LPS stimulation at 3, 12, and 24 h. Compared with the LPS group, the *PTGS2* gene expression decreased ( $P < 0.01$ ) in LPS–MEL groups. There was no difference ( $P > 0.05$ ) in the *TLR4* transcription between the LPS group and the LPS–MEL groups. Compared with the blank control group, the gene expression of most growth factors showed no change ( $P > 0.05$ ) or a downregulation ( $P < 0.05$ ) after LPS treatment at observed time points, except *TGFB3* at 12 and 24 h (**Figures 8C–G**). The gene expression of growth factors in LPS–MEL groups were generally lower ( $P < 0.05$ ) than those in the LPS group at 3 and 12 h. Other than the decreased mRNA abundance of *TGFB3* ( $P < 0.05$ ) in the LPS–MEL groups as compared with the LPS group, we found no other differences ( $P > 0.05$ ) at 24 h. The mRNA abundance of *PTGS1* was not influenced ( $P > 0.05$ ) by LPS or LPS–MEL treatment (**Figure 8H**).

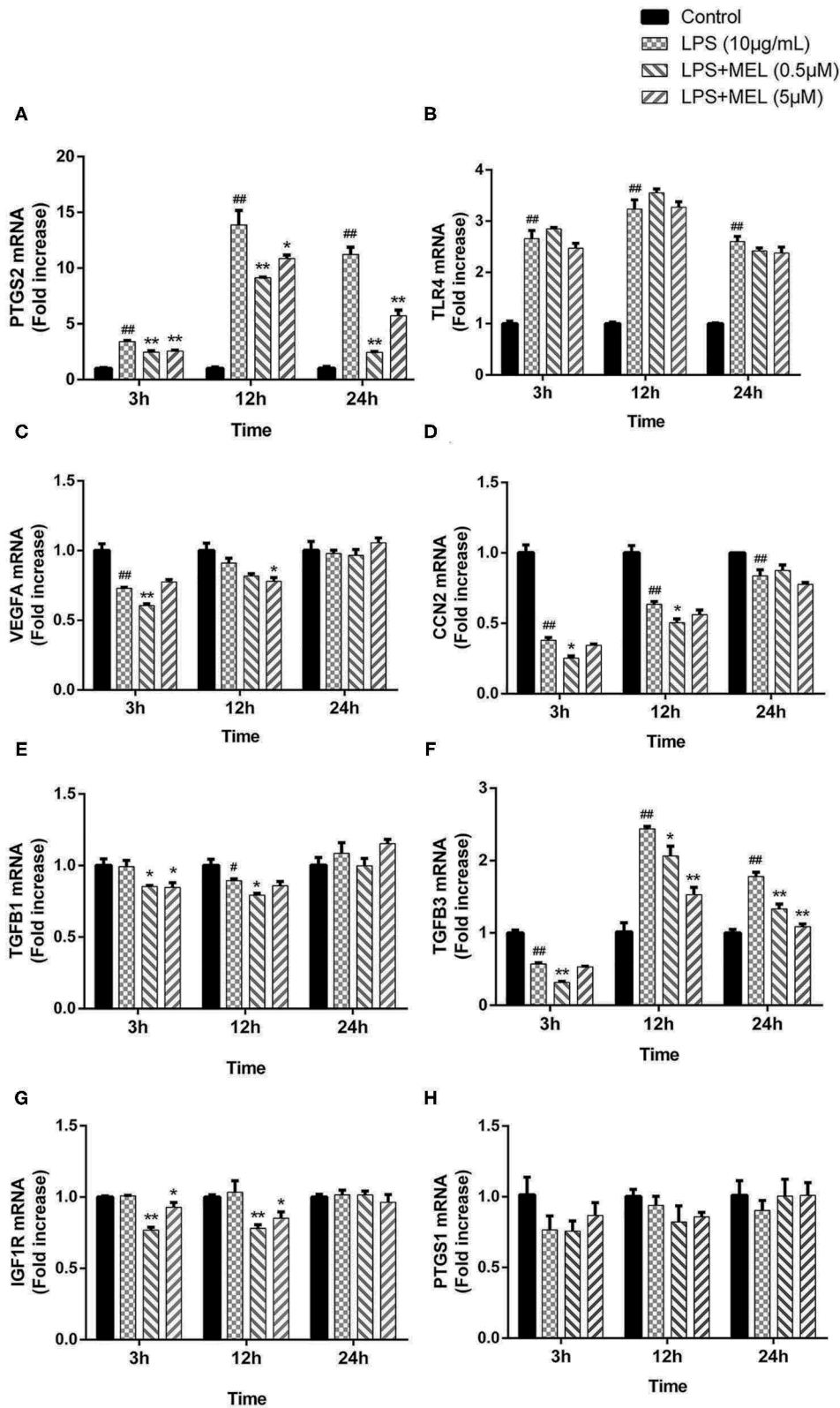


**FIGURE 8 |** The effect of meloxicam on the mRNA expressions of *PTGS2* (A), *TLR4* (B), *VEGFA* (C), *CCN2* (D), *TGFB1* (E), *TGFB3* (F), *IGF1R* (G), and *PTGS1* (H) in bovine endometrial epithelial cells stimulated with lipopolysaccharide. LPS, lipopolysaccharide; MEL, meloxicam. The cells were treated with LPS or co-treated with (Continued)

**FIGURE 8** | LPS and MEL (0.5 and 5  $\mu$ M) for 3, 12, or 24 h. The relative mRNA abundance was detected by quantitative reverse-transcription polymerase chain reaction and was analyzed by the  $2^{-\Delta\Delta CT}$  method. *ACTB* was used as the housekeeping gene. Each group was repeated three times. # $P < 0.05$ , difference compared with the control; ## $P < 0.01$ , difference compared with the control; \* $P < 0.05$ , difference compared with the LPS treatment group; \*\* $P < 0.01$ , difference compared with the LPS treatment group. All data were presented as means  $\pm$  SEM ( $n = 3$ ).

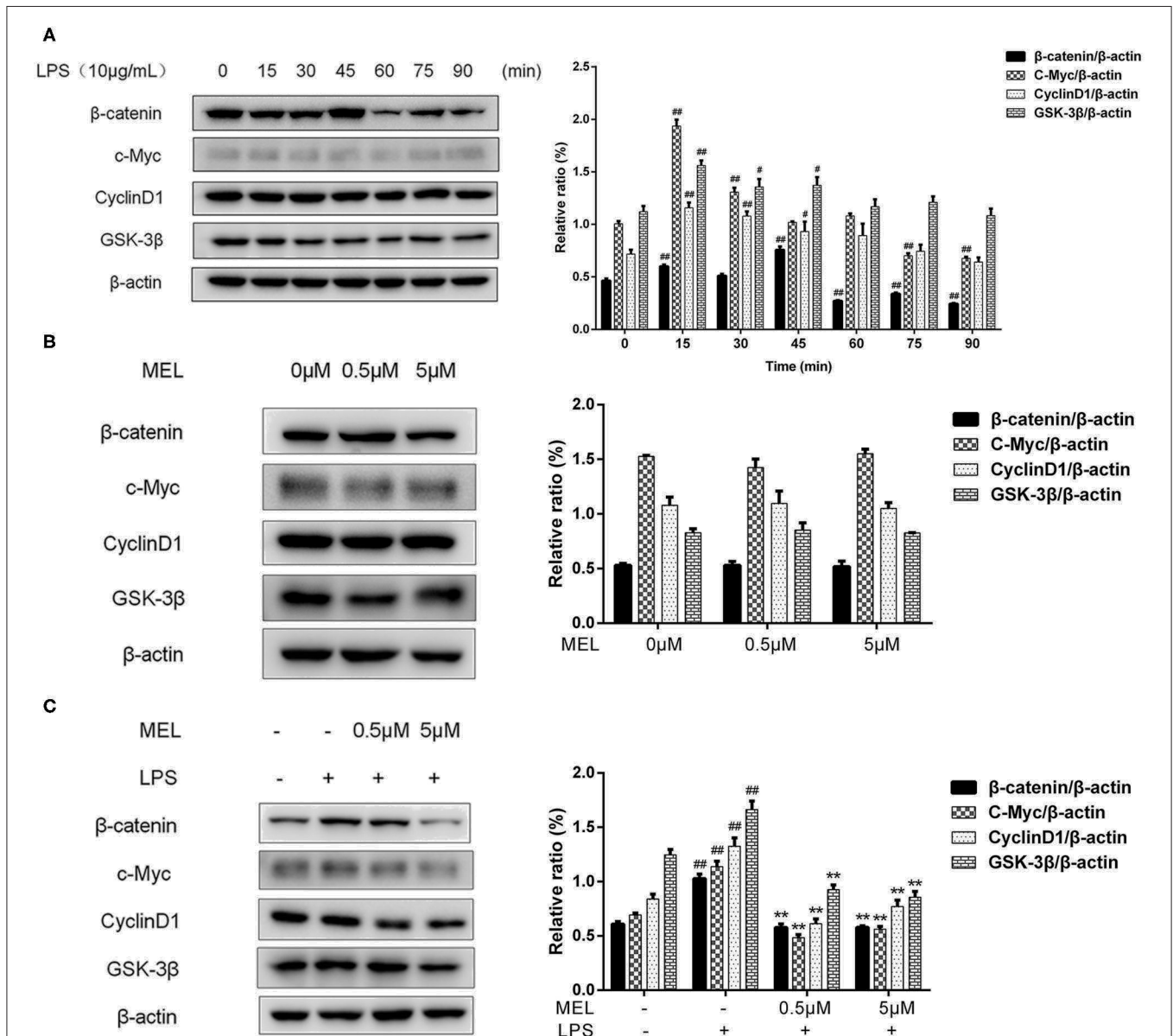
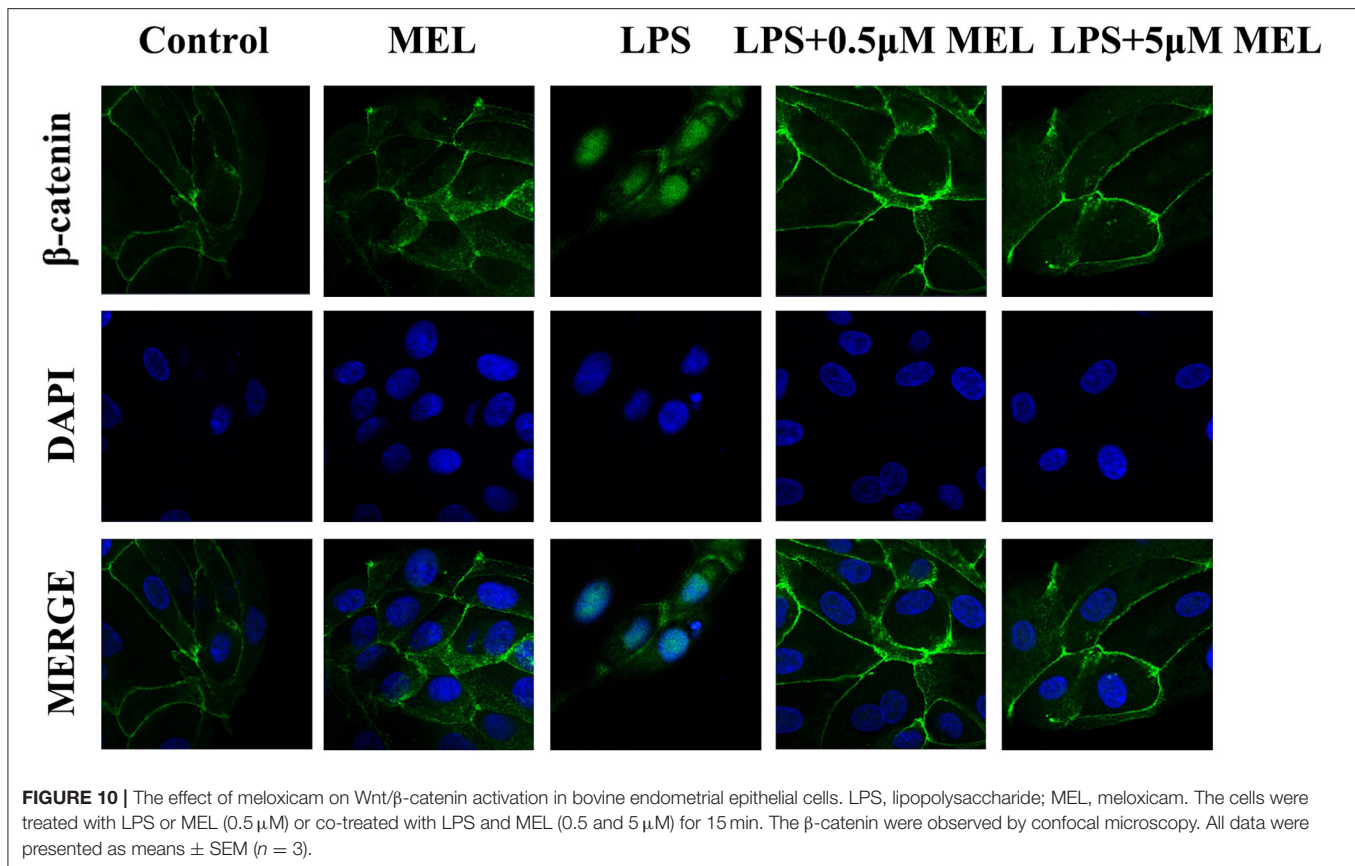


**FIGURE 9** | The effect of meloxicam on the Wnt/ $\beta$ -catenin pathway in bovine endometrial epithelial cells. The protein levels of  $\beta$ -catenin, c-Myc, cyclin D1, and GSK-3 $\beta$  were determined using western blot. The band intensity quantification was analyzed by Quantity One software.  $\beta$ -Actin was used as the internal control. LPS, lipopolysaccharide; MEL, meloxicam. **(A)** The cells were treated with LPS for 0, 15, 30, 45, 60, 75, and 90 min. **(B)** The cells were treated with MEL alone for 15 min. **(C)** The cells were treated with LPS or co-treated with LPS and MEL (0.5 and 5  $\mu$ M) for 15 min. # $P < 0.05$ , difference compared with the control; ## $P < 0.01$ , difference compared with the control; \* $P < 0.05$ , difference compared with the LPS treatment group; \*\* $P < 0.01$ , difference compared with the LPS treatment group. All data were presented as means  $\pm$  SEM ( $n = 3$ ).

## Wnt/ $\beta$ -Catenin Activation in BEECs

The effects of MEL on the protein levels of  $\beta$ -catenin, c-Myc, cyclin D1, and GSK-3 $\beta$  were detected using western blot. As

shown in **Figure 9A**, the protein level of  $\beta$ -catenin increased ( $P < 0.01$ ) at 15 and 45 min and decreased ( $P < 0.01$ ) at 60, 75, and 90 min. The levels of c-Myc and cyclin D1 increased ( $P <$



0.05) at 15 and 30 min. The level of GSK-3β increased ( $P < 0.05$ ) at 15, 30, and 45 min. Based on these results, we selected 15 min to detect the changes in the Wnt/β-catenin pathway in subsequent experiments.

MEL (0.5 and 5 μM) treatment alone did not influence ( $P > 0.05$ ) the protein levels of β-catenin, c-Myc, cyclin D1, or GSK-3β as compared with the blank control (**Figure 9B**). LPS stimulation caused an increase ( $P < 0.01$ ) in the levels of β-catenin, c-Myc, cyclin D1, and GSK-3β (**Figure 9C**). Compared with the LPS group, the levels of these proteins were lower ( $P < 0.01$ ) in the LPS-MEL groups.

### β-Catenin Distribution in BEECs

As shown in **Figure 10**, the β-catenin level on the cytomembrane in the MEL (0.5 μM) group was similar to that in the control group. In the LPS group, an increased number of β-catenin was observed to enter the nucleus. Compared with the LPS group, the amount of β-catenin in the nucleus in LPS-MEL groups seemed lower, and the β-catenin was mainly detected in the cytomembrane.

### PI3K/AKT Activation in BEECs

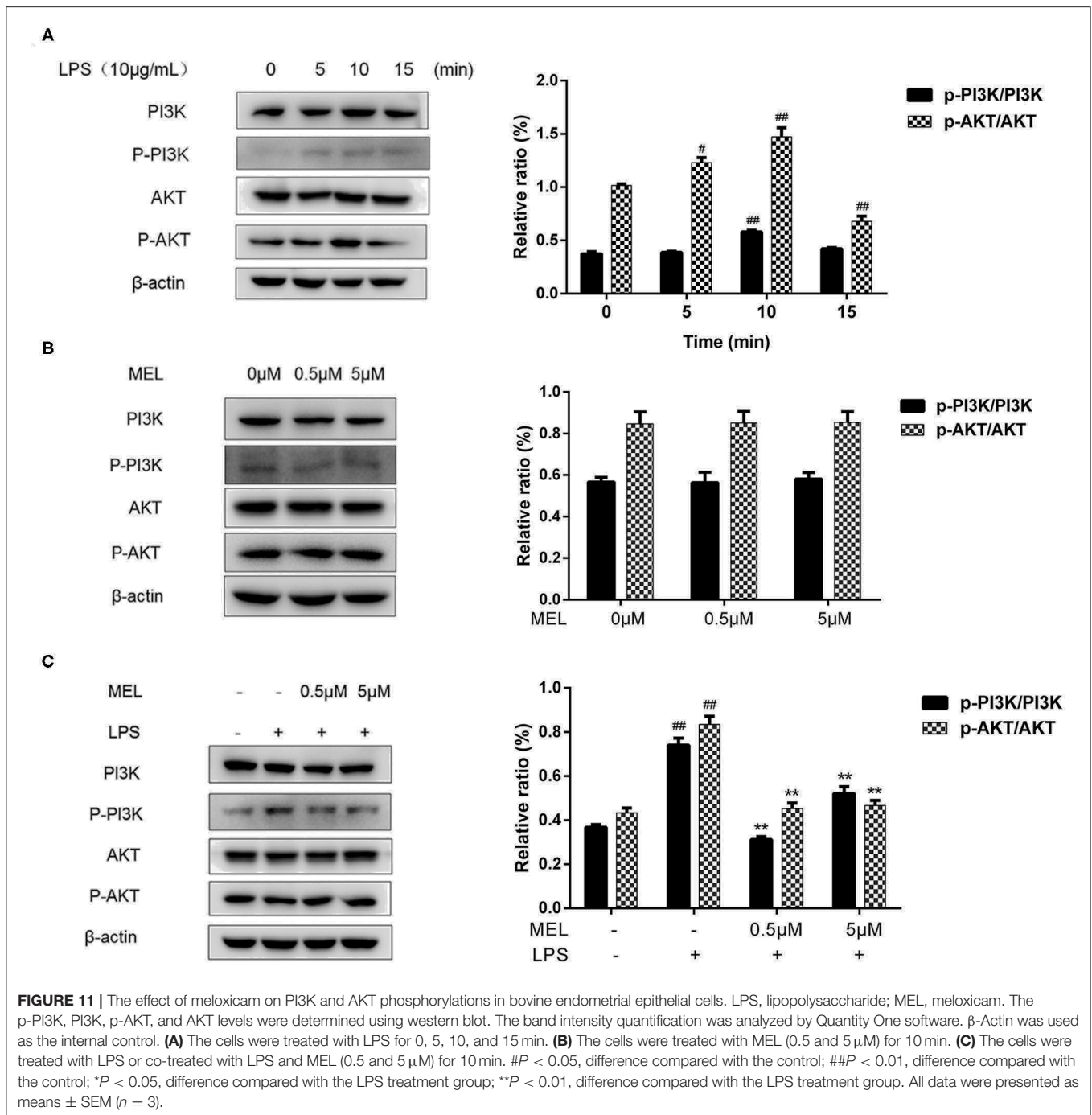
The influence of MEL on the PI3K/AKT pathway was detected using western blot and is depicted in **Figure 11A**. The phosphorylation levels of PI3K and AKT showed similar trends. The p-PI3K/PI3K ratio increased ( $P < 0.01$ ) at 10 min, whereas

the of p-AKT/AKT ratio increased ( $P < 0.05$ ) at 5 and 10 min and decreased at 15 min. Based on these results, the time point of 10 min was selected for subsequent experiments.

MEL alone (0.5 or 5 μM) showed no effect ( $P > 0.05$ ) on the PI3K/AKT pathway (**Figure 11B**). Compared with the blank control group, the phosphorylation levels of PI3K and AKT increased ( $P < 0.01$ ) in the LPS group. Compared with the LPS group, the phosphorylation levels of PI3K and AKT decreased ( $P < 0.01$ ) in the LPS-MEL groups (**Figure 11C**).

## DISCUSSION

The COX-1 and COX-2 were encoded by *PTGS1* and *PTGS2* genes, respectively. In this study, MEL reduced the *PTGS2* but not *PTGS1* transcription in BEEC stimulated with LPS, implying its preferential inhibitory effect on COX-2 over COX-1. MEL inhibited PI3K/AKT and Wnt/β-catenin pathways and the downstream c-Myc, cyclin D1, and VEGF, resulting in the cell cycle block and the downregulation of cell proliferation in LPS-stimulated BEEC. This was similar to the report that the cell survival was inhibited by MEL treatment in LPS-challenged bovine mammary epithelial cells (20). These results indicated that MEL treatment may induce tissue damage in the endometrium. Whether the character of this discovery would support or impair the elimination of bacteria from infected uterine cavity



during metritis or endometritis therapy with MEL still needs a comprehensive investigation.

The results showed that 0.5 and 5 µM MEL with or without 10 µg/ml LPS treatment had no effect on BEEC viability. By observing the cell scratch test, MEL alone had no effect on cell migration. This was consistent with the results of Goncalves et al. (27), showing that 5 µM MEL had no effect on cell viability and migration rate in adult mouse brain neural cells. When BEEC was co-treated with MEL and LPS, the cell healing rate reduced.

Similarly, Chechik et al. (28) demonstrated that MEL interfered with the normal healing process of the ruptured supraspinatus tendon in rats, which was supported by Cohen et al. (29), who found that celecoxib inhibited tendon-to-bone healing, and by Ferry et al. (30), who reported that ibuprofen had a detrimental effect on healing strength at the bone-tendon junction. The discrepancy between the result of MEL treatment alone and LPS-MEL suggested that the action of MEL on BEEC proliferation was indirect.

COX-2 is a pathological inducer, which catalyzes the synthesis of PG and participates in inflammatory reaction. Our results showed that MEL inhibited LPS-induced *PTGS2* transcription in BEEC, and many studies supported this result (31, 32). It has been reported that TLR4 mainly exists in bovine endometrial cells (6). The recognition of LPS by TLR4 activates the nuclear factor kappa-B (NF- $\kappa$ B) pathway, which promotes the transcription of proinflammatory cytokines, causing inflammatory response (33). Our results were consistent with reports that LPS promoted *TLR4* gene expression. However, MEL did not attenuate the LPS-induced *TLR4* gene expression, which may be explained by its effect on the downstream NF- $\kappa$ B pathway (34). Growth factors (VEGF, CTGF, IGFR, TGF- $\beta$ 1, and TGF- $\beta$ 3) play a regulatory role in the proliferation, differentiation, matrix repair, and remodeling of endometrial epithelial cells and stromal cells (8, 35, 36). Our result showed that MEL inhibited gene expressions of *VEGFA*, *CCN2*, *IGF1R*, *TGFBI*, and *TGFB3* in LPS-stimulated BEEC to varying degrees. VEGF and CTGF were encoded by *VEGFA* and *CCN2* genes, respectively. Quintana et al. found that MEL inhibited VEGF expression in ovarian hyperstimulation syndrome (37). Other studies have found that N-(2-cyclohexyloxy-4-nitrophenyl)-methanesulfonamide, another preferential inhibitor of COX-2 over COX-1, reduced the human pancreatic cancer cell number through inhibiting the expressions of VEGF and CTGF (38). Tolfenamic acid has been shown to inhibit the proliferation of hepatoma cells by regulating TGF- $\beta$ 1 expression (39). These reports supported the results of our experiment that MEL downregulated the mRNA abundance of *VEGFA*, *CCN2*, *IGF1R*, *TGFBI*, and *TGFB3* and inhibited the proliferation and growth of BEEC.

Wnt/ $\beta$ -catenin is involved in wound healing, uterine development, embryo implantation, and uterine involution (40, 41). Cheng et al. found that LPS activated the Wnt/ $\beta$ -catenin pathway in a rat model of pneumonia (42). Similarly, we found that the levels of  $\beta$ -catenin, c-Myc, cyclin D1, and GSK-3 $\beta$  increased after LPS stimulation. NSAIDs have been shown to inhibit GSK-3 $\beta$  protein expression and to downregulate the transcription of  $\beta$ -catenin/TCF responsive gene (43, 44). Vallee et al. (45) demonstrated that NSAIDs inhibited the Wnt/ $\beta$ -catenin pathway and alleviated inflammatory response. In this study, LPS-MEL decreased the levels of  $\beta$ -catenin, GSK-3 $\beta$ , c-Myc, and cyclin D1 and prevented  $\beta$ -catenin from entering the nucleus, indicating the inhibition of the Wnt/ $\beta$ -catenin pathway by MEL. Cyclin D1 and c-Myc are the downstream factors of the Wnt/ $\beta$ -catenin pathway and are essential for cell cycle progression (46). Our results showed that the cell cycle was arrested in the G0/G1 phase in LPS-MEL groups. In cancer studies, NSAIDs could induce cell cycle arrest, apoptosis, and angiogenesis inhibition (47). Arantes-Rodrigues et al. found that MEL reduced the proliferation of bladder cancer cells and arrested the cells in the G0/G1 phase (48). These results revealed that MEL blocked the cell cycle of BEEC through the Wnt/ $\beta$ -catenin pathway and its downstream cyclin D1 and c-Myc. In addition, TGF- $\beta$ 1 has been shown to activate the Wnt/ $\beta$ -catenin pathway (49). Our results showed that LPS-MEL reduced the

gene expression of *TGFBI*, suggesting another potential target of MEL in inhibiting the Wnt/ $\beta$ -catenin pathway.

The PI3K/AKT pathway regulates various cellular processes such as cell proliferation and differentiation (50, 51). AKT, mainly activated by PI3K, induces cell proliferation and survival (52). In accordance with previous report, we found that the phosphorylation of PI3K and AKT increased after LPS stimulation (53). Evidence has shown that NSAID inhibits the AKT signaling pathway. In the treatment of endometrial cancer, MEL has played a role through the PI3K/AKT pathway (54). Similarly, our results indicated the inhibitory effect of MEL on LPS-induced PI3K/AKT activation. Wnt/ $\beta$ -catenin and PI3K/AKT pathways are interconnected by intracellular GSK-3 $\beta$ . The phosphorylated form of AKT activates GSK-3 $\beta$ , causing the adenomatous polyposis coli/axin/GSK-3 $\beta$  complex to lose its binding ability to  $\beta$ -catenin, allowing  $\beta$ -catenin to enter the nucleus (55). NSAIDs induce GSK-3 $\beta$  phosphorylation and inhibit the phosphorylation of PI3K and AKT, so that GSK-3 $\beta$  continues to be downregulated at the phosphorylation level, and the negative feedback on PI3K/AKT pathway has a more obvious inhibitory effect (56). Moreover, IGFR has been shown to activate the PI3K/AKT pathway (57); the decreased gene expression of *IGF1R* in the LPS-MEL groups may further inhibit the activation of the PI3K/AKT pathway. Further studies are required to clarify the mechanism.

In conclusion, MEL reduced the cell proliferation, blocked the cell cycle progression, and inhibited the gene expressions of *VEGFA*, *CCN2*, *IGF1R*, *TGFBI*, and *TGFB3* in LPS-challenged BEEC. This inhibitory effect of MEL was possibly mediated by Wnt/ $\beta$ -catenin and PI3K/AKT pathways.

## DATA AVAILABILITY STATEMENT

The original contributions presented in the study are included in the article/**Supplementary Material**, further inquiries can be directed to the corresponding author/s.

## AUTHOR CONTRIBUTIONS

LC: conceptualization and methodology. YQ: data curation, writing—original draft preparation, and software. HC: visualization, software, and validation. JD and JuL: investigation. HW and CQ: supervision. JiL: supervision, writing—reviewing, and editing. All authors contributed to the article and approved the submitted version.

## FUNDING

This work was supported by the National Natural Science Foundation of China (nos. 32072937, 31672614, and 31802253), the China Postdoctoral Science Foundation (no. 2018M632398), the Natural Science Foundation of Jiangsu Province (no. BK20160062), the China Scholarship Council (no. 201908320077), the Outstanding Young

Backbone Teacher Foundation of Yangzhou University, the Priority Academic Program Development of Jiangsu Higher Education Institutions (PAPD), and the Topnotch Academic Programs Project of Jiangsu Higher Education Institutions (TAPP).

## SUPPLEMENTARY MATERIAL

The Supplementary Material for this article can be found online at: <https://www.frontiersin.org/articles/10.3389/fvets.2021.637707/full#supplementary-material>

## REFERENCES

- Lomb J, Neave HW, Weary DM, LeBlanc SJ, Huzzey JM, Keyserlingk MAG. Changes in feeding, social, and lying behaviors in dairy cows with metritis following treatment with a nonsteroidal anti-inflammatory drug as adjunctive treatment to an antimicrobial. *J Dairy Sci.* (2018) 101:4400–11. doi: 10.3168/jds.2017-13812
- Kasse FN, Fairbrother JM, Dubuc J. Relationship between *Escherichia coli* virulence factors and postpartum metritis in dairy cows. *J Dairy Sci.* (2016) 99:4656–67. doi: 10.3168/jds.2015-10094
- Sheldon IM, Price SB, Cronin J, Gilbert RO, Gadsby JE. Mechanisms of infertility associated with clinical and subclinical endometritis in high producing dairy cattle. *Reprod Domest Anim.* (2009) 44:1–9. doi: 10.1111/j.1439-0531.2009.01465.x
- Sheldon IM, Cronin JG, Healey GD, Gabler C, Heuwieser W, Strey D, et al. Innate immunity and inflammation of the bovine female reproductive tract in health and disease. *Reproduction.* (2014) 148:R41–51. doi: 10.1530/REP-14-0163
- Wathes DC, Cheng Z, Chowdhury W, Fenwick MA, Fitzpatrick R, Morris DG, et al. Negative energy balance alters global gene expression and immune responses in the uterus of postpartum dairy cows. *Physiol Genom.* (2009) 39:1–13. doi: 10.1152/physiolgenomics.00064.2009
- Fu Y, Liu B, Feng X, Liu Z, Liang D, Li F, et al. Lipopolysaccharide increases Toll-like receptor 4 and downstream Toll-like receptor signaling molecules expression in bovine endometrial epithelial cells. *Vet Immunol Immunopathol.* (2013) 151:20–7. doi: 10.1016/j.vetimm.2012.09.039
- Fan X, Krieg S, Kuo CJ, Wiegand SJ, Rabinovitch M, Druzin M.L, et al. VEGF blockade inhibits angiogenesis and reepithelialization of endometrium. *FASEB J.* (2008) 22:3571–80. doi: 10.1096/fj.08-111401
- Maybin JA, Barcroft J, Thiruchelvam U, Hirani N, Jabbour HN, Critchley HO. The presence and regulation of connective tissue growth factor in the human endometrium. *Hum Reprod.* (2012) 27:1112–21. doi: 10.1093/humrep/der476
- Evans J, Infusini G, McGovern J, Cuttle L, Webb A, Nebl T, et al. Menstrual fluid factors facilitate tissue repair: identification and functional action in endometrial and skin repair. *FASEB J.* (2019) 33:584–605. doi: 10.1096/fj.201800086R
- Vizzini A, Di Falco F, Parrinello D, Sanfratello MA, Cammarata M. Transforming growth factor beta (TGF-beta) gene expression is induced in the inflammatory reaction of Ciona intestinalis. *Dev Comp Immunol.* (2016) 55:102–10. doi: 10.1016/j.dci.2015.10.013
- Fan X, Krieg S, Hwang JY, Dhal S, Kuo CJ, Lasley BL, et al. Dynamic regulation of Wnt7a expression in the primate endometrium: implications for postmenstrual regeneration and secretory transformation. *Endocrinology.* (2012) 153:1063–9. doi: 10.1210/en.2011-1826
- Goad J, Ko YA, Kumar M, Syed SM, Tanwar PS. Differential Wnt signaling activity limits epithelial gland development to the anti-mesometrial side of the mouse uterus. *Dev Biol.* (2017) 423:138–51. doi: 10.1016/j.ydbio.2017.01.015
- Tepekoy F, Akkoyunlu G, Demir R. The role of Wnt signaling members in the uterus and embryo during pre-implantation and implantation. *J Assist Reprod Genet.* (2014) 32:337–46. doi: 10.1007/s10815-014-0409-7
- Daniels DL, Weis WI. Beta-catenin directly displaces Groucho/TLE repressors from Tcf/Lef in Wnt-mediated transcription activation. *Nat Struct Mol Biol.* (2005) 12:364–71. doi: 10.1038/nsmb912
- Liu X, Zhang L, Liu Y, Cui J, Che S, An X, et al. Circ-8073 regulates CEP55 by sponging miR-449a to promote caprine endometrial epithelial cells proliferation via the PI3K/AKT/mTOR pathway. *Biochim Biophys Acta Mol Cell Res.* (2018) 1865:1130–47. doi: 10.1016/j.bbamcr.2018.05.011
- Zhu H, Jiang Y, Pan Y, Shi L, Zhang S. Human menstrual blood-derived stem cells promote the repair of impaired endometrial stromal cells by activating the p38 MAPK and AKT signaling pathways. *Reprod Biol.* (2018) 18:274–81. doi: 10.1016/j.repbio.2018.06.003
- Meac A, Jarb B, Jobb C. Attitudes of cattle veterinarians and animal scientists to pain and painful procedures in Brazil. *Prev Vet Med.* (2020) 177:104909–17. doi: 10.1016/j.prevetmed.2020.104909
- Laven R, Chambers P, Stafford K. Using non-steroidal anti-inflammatory drugs around calving: maximizing comfort, productivity and fertility. *Vet J.* (2012) 192:8–12. doi: 10.1016/j.tvjl.2011.10.023
- Beretta C, Garavaglia G, Cavalli M. COX-1 and COX-2 inhibition in horse blood by phenylbutazone, flunixin, carprofen and meloxicam: an *in vitro* analysis. *Pharmacol Res.* (2005) 52:302–6. doi: 10.1016/j.phrs.2005.04.004
- Caldeira MO, Bruckmaier RM, Wellnitz O. Meloxicam affects the inflammatory responses of bovine mammary epithelial cells. *J Dairy Res.* (2019) 102:10277–90. doi: 10.3168/jds.2019-16630
- Dong J, Qu Y, Li J, Cui L, Wang Y, Lin J, et al. Cortisol inhibits NF-κB and MAPK pathways in LPS activated bovine endometrial epithelial cells. *Int Immunopharmacol.* (2018) 56:71–7. doi: 10.1016/j.intimp.2018.01.021
- Maslanka T. Effect of dexamethasone and meloxicam on counts of selected T lymphocyte subpopulations and NK cells in cattle - *In vivo* investigations. *Res Vet Sci.* (2014) 96:338–46. doi: 10.1016/j.rvsc.2014.02.006
- Maslanka T, Jaroszewski JJ, Markiewicz W, Jasička A, Ziolkowski H, Jedrzkiewicz D. Effects of dexamethasone and meloxicam on bovine CD25+ CD8+ and CD25- CD8+ T cells - *in vitro* study. *Res Vet Sci.* (2013) 94:662–74. doi: 10.1016/j.rvsc.2012.12.005
- Maslanka T, Jaroszewski JJ. *In vitro* studies on the influence of dexamethasone and meloxicam on bovine WC<sup>1+</sup> γδ T cells. *Vet Immunol Immunopathol.* (2013) 151:248–62. doi: 10.1016/j.vetimm.2012.11.015
- Cui L, Wang H, Lin J, Wang Y, Dong J, Li J, et al. Progesterone inhibits inflammatory response in E.coli- or LPS-stimulated bovine endometrial epithelial cells by NF-κB and MAPK pathways. *Dev Comp Immunol.* (2020) 105:103568–78. doi: 10.1016/j.dci.2019.103568
- Livak KJ, Schmittgen TD. Analysis of relative gene expression data using real-time quantitative PCR and the 2<sup>-ΔΔCT</sup> Method. *Methods.* (2001) 25:402–8. doi: 10.1006/meth.2001.1262
- Goncalves MB, Williams EJ, Yip P, Yanez-Munoz RJ, Williams G, Doherty P. The COX-2 inhibitors, meloxicam and nimesulide, suppress neurogenesis in the adult mouse brain. *Br J Pharmacol.* (2010) 159:1118–25. doi: 10.1111/j.1476-5381.2009.00618.x
- Chechik O, Dolkart O, Mozes G, Rak O, Alhajajra F, Maman E. Timing matters: NSAIDs interfere with the late proliferation stage of a repaired rotator cuff tendon healing in rats. *Arch Orthopaed Traumat Surg.* (2014) 134:515–20. doi: 10.1007/s00402-014-1928-5
- Cohen DB, Kawamura S, Ehteshami JR, Rodeo SA. Indomethacin and celecoxib impair rotator cuff tendon-to-bone healing. *Am J Sports Med.* (2006) 34:362–9. doi: 10.1177/0363546505280428
- Ferry ST, Dahners LE, Afshari HM, Weinhold PS. The effects of common anti-inflammatory drugs on the healing rat patellar tendon. *Am J Sports Med.* (2007) 35:1326–33. doi: 10.1177/0363546507301584
- Li J, Chen X, Dong X, Xu Z, Jiang H, Sun X. Specific COX-2 inhibitor, meloxicam, suppresses proliferation and induces apoptosis in human HepG2 hepatocellular carcinoma cells. *J Gastroenterol Hepatol.* (2006) 21:1814–20. doi: 10.1111/j.1440-1746.2006.04366.x
- Li H, Luo Y, Xu Y, Yang L, Hu C, Chen Q, et al. Meloxicam improves cognitive impairment of diabetic rats through COX2-PGE2-EPs-cAMP/pPKA pathway. *Mol Pharm.* (2018) 15:4121–31. doi: 10.1021/acs.molpharmaceut.8b00532
- Yin P, Zhang Z, Li J, Shi Y, Jin N, Zou W, et al. Ferulic acid inhibits bovine endometrial epithelial cells against LPS-induced inflammation via suppressing NF-κB and MAPK pathway. *Res Vet Sci.* (2019) 126:164–9. doi: 10.1016/j.rvsc.2019.08.018

34. Hassan MH, Ghobara MM. Antifibrotic effect of meloxicam in rat liver: role of nuclear factor kappa B, proinflammatory cytokines, and oxidative stress. *Naunyn-Schmiedeberg's Arch Pharmacol.* (2016) 389:971–83. doi: 10.1007/s00210-016-1263-1
35. Sharkey AM, Day K, McPherson A, Malik S, Licence D, Smith SK, et al. Vascular endothelial growth factor expression in human endometrium is regulated by hypoxia. *J Clin Endocrinol Metab.* (2000) 85:402–9. doi: 10.1210/jc.85.1.402
36. Schiller M, Javelaud D, Mauviel A. TGF-beta-induced SMAD signaling and gene regulation: consequences for extracellular matrix remodeling and wound healing. *J Dermatol Sci.* (2004) 35:83–92. doi: 10.1016/j.jdermsci.2003.12.006
37. Quintana R, Kopcow L, Marconi G, Young E, Yovanovich C, Paz DA. Inhibition of cyclooxygenase-2 (COX-2) by meloxicam decreases the incidence of ovarian hyperstimulation syndrome in a rat model. *Fertil Steril.* (2008) 90(Suppl. 4):1511–6. doi: 10.1016/j.fertnstert.2007.09.028
38. Youns M, Efferth T, Hoheisel JD. Transcript profiling identifies novel key players mediating the growth inhibitory effect of NS-398 on human pancreatic cancer cells. *Eur J Pharmacol.* (2011) 650:170–7. doi: 10.1016/j.ejphar.2010.10.026
39. Sun J, Tao R, Mao T, Feng Z, Guo Q, Zhang X. The involvement of lipid raft pathway in suppression of TGFβ-mediated metastasis by tofenamic acid in hepatocellular carcinoma cells. *Toxicol Appl Pharmacol.* (2019) 380:114696–708. doi: 10.1016/j.taap.2019.114696
40. Sonderegger S, Pollheimer J, Knofler M. Wnt signalling in implantation, decidualisation and placental differentiation—review. *Placenta.* (2010) 31:839–47. doi: 10.1016/j.placenta.2010.07.011
41. Chen JG, Chen T, Ding Y, Han L, Zhou FY, Chen WZ, et al. Baicalin can attenuate the inhibitory effects of mifepristone on Wnt pathway during peri-implantation period in mice. *J Steroid Biochem Mol Biol.* (2015) 149:11–6. doi: 10.1016/j.jsbmb.2014.11.023
42. Cheng L, Zhao Y, Qi D, Li W, Wang D. Wnt/beta-catenin pathway promotes acute lung injury induced by LPS through driving the Th17 response in mice. *Biochem Biophys Res Commun.* (2018) 495:1890–5. doi: 10.1016/j.bbrc.2017.12.058
43. Li T, Zhong J, Dong X, Xiu P, Wang F, Wei H, et al. Meloxicam suppresses hepatocellular carcinoma cell proliferation and migration by targeting COX-2/PGE2-regulated activation of the beta-catenin signaling pathway. *Oncol Rep.* (2016) 35:3614–22. doi: 10.3892/or.2016.4764
44. Dihlmann S, Siermann A, Doeberitz MvK. The nonsteroidal anti-inflammatory drugs aspirin and indomethacin attenuate beta-catenin TCF-4 signaling. *Oncogene.* (2001) 20:645–53. doi: 10.1038/sj.onc.1204123
45. Vallee A, Lecarpentier Y, Vallee JN. Targeting the canonical WNT/beta-catenin pathway in cancer treatment using non-steroidal anti-inflammatory drugs. *Cells.* (2019) 8:700–26. doi: 10.3390/cells8070726
46. Olmeda D, Castel S, Vilaro S, Cano A. Beta-catenin regulation during the cell cycle: implications in G2/M and apoptosis. *Mol Biol Cell.* (2003) 14:2844–60. doi: 10.1091/mbc.e03-01-0865
47. Thun MJ, Henley SJ, Patrono C. Nonsteroidal anti-inflammatory drugs as anticancer agents: mechanistic, pharmacologic, and clinical issues. *J Natl Cancer Inst.* (2002) 94:252–66. doi: 10.1093/jnci/94.4.252
48. Arantes-Rodrigues R, Pinto-Leite R, Ferreira R, Neuparth MJ, Pires MJ, Gaivao I, et al. Meloxicam in the treatment of *in vitro* and *in vivo* models of urinary bladder cancer. *Biomed Pharmacother.* (2013) 67:277–84. doi: 10.1016/j.biopha.2013.01.010
49. Baarsma HA, Spanjer AI, Haitsma G, Engelbertink LH, Meurs H, Jonker MR, et al. Activation of WNT/β-catenin signaling in pulmonary fibroblasts by TGF-β1 is increased in chronic obstructive pulmonary disease. *PLoS ONE.* (2011) 6:e25450. doi: 10.1371/journal.pone.0025450
50. Shi X, Ran L, Liu Y, Zhong SH, Zhou PP, Liao MX, et al. Knockdown of hnRNP A2/B1 inhibits cell proliferation, invasion and cell cycle triggering apoptosis in cervical cancer via PI3K/AKT signaling pathway. *Oncol Rep.* (2018) 39:939–50. doi: 10.3892/or.2018.6195
51. Carnero A, Aparicio CB, Renner O, Link W, Leal JF. The PTEN/PI3K/AKT signalling pathway in cancer, therapeutic implications. *Curr Cancer Drug Targets.* (2008) 8:187–98. doi: 10.2174/156800908784293659
52. Dong J, Li J, Li J, Cui L, Meng X, Qu Y, et al. The proliferative effect of cortisol on bovine endometrial epithelial cells. *Reprod Biol Endocrinol.* (2019) 17:97. doi: 10.1186/s12958-019-0544-1
53. Zheng P, Tian X, Zhang W, Yang Z, Zhou J, Zheng J, et al. Rhein suppresses neuroinflammation via multiple signaling pathways in LPS-stimulated BV2 microglia cells. *Evid Based Complement Alternat Med.* (2020) 2020:1–12. doi: 10.1155/2020/7210627
54. Kanayama S, Yamada Y, Kawaguchi R, Tsuji Y, Haruta S, Kobayashi H. Hepatocyte growth factor induces anoikis resistance by up-regulation of cyclooxygenase-2 expression in uterine endometrial cancer cells. *Oncol Rep.* (2008) 19:117–22. doi: 10.3892/or.19.1.117
55. Covey TM, Edes K, Coombs GS, Virshup DM, Fitzpatrick FA. Alkylation of the tumor suppressor PTEN activates Akt and beta-catenin signaling: a mechanism linking inflammation and oxidative stress with cancer. *PLoS ONE.* (2010) 5:e13545–56. doi: 10.1371/journal.pone.0013545
56. Moore SF, Bosch MT, Hunter RW, Sakamoto K, Poole AW, Hers I. Dual regulation of glycogen synthase kinase 3 (GSK3)α/β by protein kinase C (PKC)α and Akt promotes thrombin-mediated integrin α<sub>IIb</sub>/β<sub>3</sub> activation and granule secretion in platelets. *J Biol Chem.* (2013) 288:3918–28. doi: 10.1074/jbc.M112.429936
57. Zoumaro AD, Ding V, Foong LY, Choo A, Heck AJ, Munoz J. Investigating the role of FGF-2 in stem cell maintenance by global phosphoproteomics profiling. *Proteomics.* (2011) 11:3962–71. doi: 10.1002/pmic.201100048

**Conflict of Interest:** The authors declare that the research was conducted in the absence of any commercial or financial relationships that could be construed as a potential conflict of interest.

Copyright © 2021 Cui, Qu, Cai, Wang, Dong, Li, Qian and Li. This is an open-access article distributed under the terms of the Creative Commons Attribution License (CC BY). The use, distribution or reproduction in other forums is permitted, provided the original author(s) and the copyright owner(s) are credited and that the original publication in this journal is cited, in accordance with accepted academic practice. No use, distribution or reproduction is permitted which does not comply with these terms.